New $Li_{2-x}Cu_xFeS_2$ ($0 \le x \le 1$) and Cu_xFeS_2 ($\sim 0.25 \le x \le 1$) phases

Rosamaría Fong and J. R. Dahn
Materials Science, Moli Energy Limited, 3958 Myrtle Street, Burnaby, British Columbia, Canada V5C 4G2

R. J. Batchelor, F. W. B. Einstein, and C. H. W. Jones
Department of Chemistry, Simon Fraser University, Burnaby, British Columbia, Canada V5A 1S6
(Received 19 September 1988)

$Li_{2-x}Cu_xFeS_2$ forms a solid solution for $0 \le x \le 1$. The crystal structures of $LiCuFeS_2$ [$a=3.807(2)$ Å and $c=6.352(1)$ Å] and $Li_{1-\delta}CuFeS_2$, where $\delta=0.35$ [$a=3.772(2)$ Å and $c=6.265(2)$ Å] have been determined by single-crystal x-ray diffraction. Both structures, space group $P\bar{3}m1$, have hexagonal close-packed layers of sulfur with one formula unit per cell. In $LiCuFeS_2$ the iron and copper atoms appear to equally and randomly fill all of the tetrahedral sites between two sulfur planes (layer II). The lithium atoms occupy the octahedral sites between the adjacent sulfur planes (layer I). When lithium atoms are removed from this compound (i.e., $Li_{\sim 0.65}CuFeS_2$), some of the copper atoms in layer II move to tetrahedral sites of layer I. When all the lithium atoms are removed, a new hexagonal Cu_xFeS_2 phase ($\sim 0.25 \le x \le 1$) forms. Differential scanning calorimetry shows that this phase is metastable. Upon heating, phase transitions to chalcopyrite and pyrite occur.

INTRODUCTION

Many lithium-iron-sulfide phases form during the charge and discharge of Li/FeS_2 high-temperature secondary batteries. Among these are $Li_3Fe_2S_4$ and Li_2FeS_2.[1] Although little is known about $Li_3Fe_2S_4$, Li_2FeS_2 has been studied extensively structurally,[2] electrochemically,[3,4] and by Mössbauer spectroscopy.[5] Recently, Li_2FeS_2 has been found as an intermediate phase which forms at low temperature during discharge of a Li/FeS_2 cell.[4]

Some of the lithium atoms in Li_2FeS_2 can be substituted with copper to form $Li_{4/3}Cu_{2/3}FeS_2$.[5,6] X-ray diffraction and Mössbauer spectroscopy show that these hexagonal compounds are structurally related.[5] Both of these phases are poor conductors,[6] but the conductivity of the copper substituted phase is higher than Li_2FeS_2 by two orders of magnitude. This is desirable as it decreases the internal resistance of the battery electrodes.

Here, $Li_{4/3}Cu_{2/3}FeS_2$ was synthesized by reacting stoichiometric amounts of lithium with pyrite (FeS_2), and chalcopyrite ($CuFeS_2$). The powder x-ray diffraction pattern can be indexed with a hexagonal unit cell, whose lattice parameters are in agreement with those previously reported. This copper substituted phase is a member of the solid solution $Li_{2-x}Cu_xFeS_2$ where $0 \le x \le 1$. We find that lithium can be removed from these materials electrochemically or by using chemical methods, to make new hexagonal Cu_xFeS_2 phases. The structure of $LiCuFeS_2$ and the chemically delithiated derivative $Li_{\sim 0.65}CuFeS_2$ were determined by single-crystal x-ray diffraction. Finally, the thermal stability of the Cu_xFeS_2 phase is studied by differential scanning calorimetry.

EXPERIMENTAL

The starting materials, chalcopyrite ($CuFeS_2$) and pyrite (FeS_2) (Teck Mining Corp., 99.8% pure and 99.7% pure, respectively) used in the preparations of $Li_{2-x}Cu_xFeS_2$, where $x=0$, $\frac{1}{4}$, $\frac{2}{3}$, and 1, were natural minerals which had been ground to a powder of less than 45 μm in size. Metal analysis showed copper (0.2%) as a major impurity in pyrite, and aluminum and calcium to be present in both minerals in trace amounts.

Chemical lithiation (lithium napthalide in tetrahydrofuran followed by heating to 800 °C) and delithiation (I_2 in acetonitrile) of $Li_{2-x}Cu_xFeS_2$ ($0 \le x \le 1$) phases for use in powder x-ray diffraction studies and cathode fabrication proceeded analogously to those in the Li_2FeS_2 system.[4] The procedures for cathode preparation, cell construction, electrochemical measurements, powder x-ray diffraction, and differential scanning calorimetry have been given elsewhere.[4] Structure determination by single-crystal x-ray diffraction proceeded as described previously.[2]

Crystals of $LiCuFeS_2$ were prepared by mixing stoichiometric amounts of Li_2S (Alfa, 99% pure), Fe (Alfa, 99.9% pure), Cu (Alfa, 99.9% pure), and $CuFeS_2$ in a helium-filled glove box. The powders were mixed and heated to 800 °C under the same conditions used previously in the preparation of lithiated materials.[4] After heating, the sample was allowed to cool over a period of 8 h to room temperature. The product had a golden metallic luster.

The sample (49.916 g) showed a weight loss of 0.6%. Assuming that the loss can be accounted for by the loss of lithium, this is equivalent to, at most, $x=0.204$ in $Li_{1-x}CuFeS_2$. But since heating was carried out in a

TABLE I. Crystal data acquisition and refinement parameters of $LiCuFeS_2$ and $Li_{\sim 0.65}CuFeS_2$.

Compound	$LiCuFeS_2$	$Li_{\sim 0.65}CuFeS_2$
Space group	$P\bar{3}m1$	$P\bar{3}m1$
a (Å)	3.807(2)	3.772(2)
c (Å)	6.352(1)	6.265(2)
U (Å^3)	79.7	77.2
$\mu_{Mo K\alpha}$ (cm^{-1})	122.1	126.0
ρ (g/cm^3)	3.97	4.05
Z	1	1
FW (g/mol)	190.45	184.20
Crystal dimensions (mm^3)	0.18×0.15×0.15	0.31×0.24×0.24
Transmission	0.67 to 1.00[a]	0.099 to 0.211[b]
Scan mode	$\omega-2\Theta$	$\omega-2\Theta$
Scan width (deg)	$1.1+0.35\tan\Theta$	$2.9+0.35\tan\Theta$
Scan speeds (deg/min)	0.96 to 5.49	2.75
$2\Theta_{max}$ (deg)	100	60
No. of reflections	363	110
	[305($I \ge 2.5\sigma I$)]	[108($I \ge 2.5\sigma I$)]
Refined variables	9	13
R_f[c]	0.033	0.044
R_{wf}[d]	0.043	0.055
GOF[e]	2.01	1.82
Weights[f]	$k=0.0002$	$k=0.0008$
Final difference peak (e/Å^3)	4.8(3)[g]	0.8(3)

[a]Data corrected empirically for absorption after Ref. 11 (relative transmission coefficients given).
[b]Data corrected analytically for absorption after Ref. 12.
[c]$R_f = \sum(|F_0|-|F_c|)/\sum|F_0|$; for observed data [$I \ge 2.5\sigma(I)$].
[d]$R_{wf} = (\sum[w(|F_0|-|F_c|)^2]/\sum wF_0^2)^{1/2}$; for observed data [$I \ge 2.5\sigma(I)$].
[e]Goodness of fit, GOF$=(\sum[w(|F_0|-|F_c|)^2]$/degrees of freedom$)^{1/2}$.
[f]$w = |\sigma^2(F)+kF^2|^{-1}$.
[g]This peak occurs on the three-fold axis at ($\frac{1}{3}$, $\frac{2}{3}$, 0.29596) and is 0.49 Å from Fe. Similarly, the second largest difference peak [1.6(3) e/Å^3] occurs 0.53 Å from S at ($\frac{2}{3}$, $\frac{1}{3}$, 0.32948). While the amplitudes of these peaks are significant, the good agreement (3.3%) and favorable observation/variable ratio indicates the overall soundness of this model; however, the possibility of twinning, a superstructure, disorder, or some combination of these cannot be excluded as candidates for a more refined analysis.

continuous flow of argon, under unsealed conditions, it is possible that the weight loss may also involve sulfur evaporation. Powder x-ray diffraction of the bulk sample showed the material to be a single phase, and lattice constants [$a=3.815(1)$ Å, $c=6.362(3)$ Å] to be in agreement with those measured on the single-crystal selected. The composition of the product is nevertheless assumed to be $LiCuFeS_2$, and in no event is $x<0.204$ in $Li_{1-x}CuFeS_2$.

Crystals of $Li_{\sim 0.65}CuFeS_2$ were obtained by treating crystalline $LiCuFeS_2$ with a stoichiometric amount of iodine in acetonitrile. After considerable effort, a single crystal was selected, mounted in a 0.5-mm diameter glass capillary tube, sealed with epoxy in the glove box, and subsequently flame sealed. The broad diffraction maxima for this crystal indicate that the delithiation process degrades the crystal quality. Attempts to prepare single crystals of $CuFeS_2$ by an analogous method yielded only microcrystalline material.

Table I summarizes the crystal data acquisition and refinement parameters. Major features of the final difference map (see Table I) of these structures were maxima and minima occurring near the Fe and S. Computations were performed with complex scattering factors for neutral atoms[7] using programs from the NRC-VAX crystal structure system.[8]

RESULTS AND DISCUSSION

The $Li_{2-x}Cu_xFeS_2$ phase, where $x=0$, $\frac{1}{4}$, $\frac{2}{3}$, and 1, was prepared. Over this range of composition, the copper substituted phase forms a solid solution. Powder x-ray diffraction patterns show that these compounds can be indexed with a hexagonal unit cell. Figure 1 shows the variation of the lattice parameters with x. As the amount of copper substituted for lithium increases, the a axis decreases while the c axis increases. The lattice parameters for $Li_{4/3}Cu_{2/3}FeS_2$ [$a=3.836(2)$ Å and $c=6.333(3)$ Å] are in good agreement with those reported by Melandres *et al.*[5]

The crystal structure of $LiCuFeS_2$ is isostructural with Li_2FeS_2 (Ref. 2), Cu replacing Li in tetrahedral holes in one layer shared equally and randomly with Fe [see Fig. 2(a)]. The refined occupancy [1.055(7)] for an iron atom in this site is consistent with 50% occupancy by both Cu and Fe. The spacing between sulfur layers separated by Cu/Fe is 3.228(2) Å, while for those separated by Li the

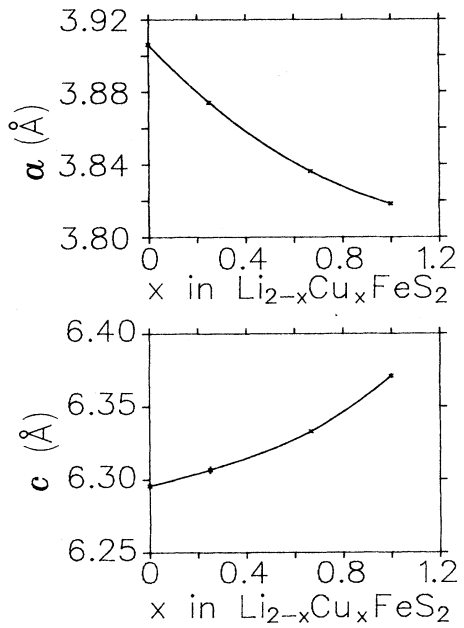

FIG. 1. Variation of the lattice parameters a and c in $Li_{2-x}Cu_xFeS_2$ with x.

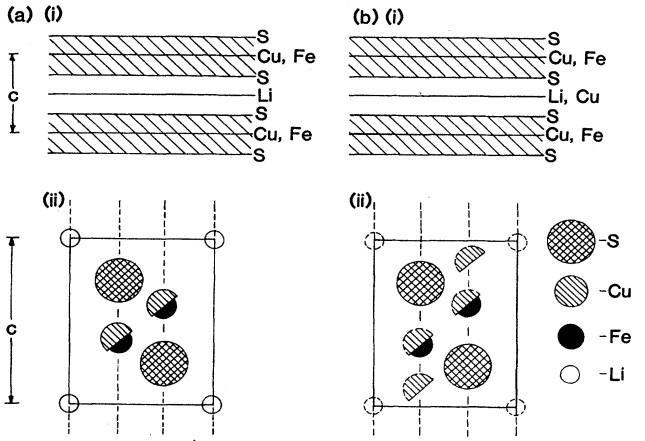

FIG. 2. Schematic diagrams of the structures: (a) $LiCuFeS_2$ and (b) $Li_{1-\delta}CuFeS_2$, where $\delta=0.35$. (i) Schematic diagrams of the layered structures, and (ii) the (110) projection of the unit cells of these structures. (A solid circle represents 100% occupancy of an atom at a site; a semicircle represents 50% occupancy of an atom at a site; a dashed circle perimeter represents partial occupancy of an atom at a site.)

spacing is 3.124(2) Å. The latter value is comparable to the analogous interlayer spacing in Li_2FeS_2 (Ref. 2) [3.133(2) Å], while the former, as a result of Cu substitution for Li, is significantly greater [3.160(2) Å in Li_2FeS_2]. The structural parameters are summarized in Table II.

When lithium was removed from the $Li_{2-x}Cu_xFeS_2$ phase, for $x=\frac{1}{4}$, $\frac{2}{3}$, and 1, either chemically using I_2/AN or electrochemically, a well-defined layered Cu_xFeS_2 phase forms ($\sim 0.25 \leq x \leq 1$) whose varying powder x-ray diffraction patterns can be indexed with a hexagonal unit cell (Fig. 3). Since diffraction peaks of the Cu_xFeS_2 phase were very broad and weak, the more crystalline partially delithiated compound was studied.

The diffraction pattern of $Li_{\sim 0.65}CuFeS_2$ was indexed on a similar hexagonal cell (Table I). These lattice constants are thought to describe the unit cell of a substructure. The structure derives from that of $LiCuFeS_2$ by the reduction of the observed electron density in the previous Fe/Cu sites of one layer and incidence of new electron density in the tetrahedral sites of the layer previously occupied only by octahedral Li. Copper atoms are known to be mobile in intercalation compounds such as $Cu_yMo_6S_8$.[9] Independently refined occupancies of the metal atom sites (Table III) could suggest similar migration of Cu from one layer to the other concomittant with removal of Li from the latter layer. Figure 2(b) shows a schematic diagram of the substructure, and a projection in the (110) plane. Table III summarizes the structural parameters of $Li_{\sim 0.65}CuFeS_2$.

Figure 4 compares the first recharge of cells assembled with $LiCuFeS_2$ and Li_2FeS_2 cathodes. The voltage profile of Li/$LiCuFeS_2$ cells shows a gradual variation with x in Li_xCuFeS_2. For Li/Li_2FeS_2 cells, a plateau at 2.5 V is observed. As previously reported,[4] beyond 2.5 V, Li_2FeS_2 disproportionates to nonstoichiometric FeS and S. In contrast, when lithium is removed from $LiCuFeS_2$, the copper atoms diffuse into the tetrahedral sites of the lithium layer. The hexagonal framework of $LiCuFeS_2$ is retained, and the layered Cu_xFeS_2 phase (where $x=1$) forms. Figure 4(a) shows that when a Li/$LiCuFeS_2$ cell is recharged to 3.4 V, approximately $\frac{3}{4}$ of the lithium in $LiCuFeS_2$ is removed. In contrast, when delithiation

TABLE II. Atomic positions in $LiCuFeS_2$.

Atom	Occupancy	x	y	z	U_{11} (Å^2)	U_{33} (Å^2)	U_{iso} (Å^2)
Fe/(Cu)[a]	1.055(8)	$\frac{1}{3}$	$\frac{2}{3}$	0.37327(8)	0.0150(2)	0.0196(3)	
S	1	$\frac{2}{3}$	$\frac{1}{3}$	0.24587(12)	0.0115(3)	0.0130(3)	
Li	1	0	0	0			0.032(3)

[a]The electron density at this site was modeled with the scattering factor for neutral iron. The refined occupancy is consistent with the statistical average of 50 at. % Cu and 50 at. % Fe.

TABLE III. Atomic positions in $Li_{\sim 0.65}CuFeS_2$.

Atom	Occupancy	x	y	z	U_{11} (Å^2)	U_{33} (Å^2)	U_{iso} (Å^2)
Fe/(Cu)[a]	0.869(13)	$\frac{1}{3}$	$\frac{2}{3}$	0.37131(19)	0.0139(6)	0.0213(8)	
Cu	0.145(7)	$\frac{1}{3}$	$\frac{2}{3}$	0.1300(12)			0.020(29)
S	1	$\frac{2}{3}$	$\frac{1}{3}$	0.25114(29)	0.0127(9)	0.0228(11)	
Li	0.90(18)	0	0	0			0.063(17)

[a]The electron density at this site was modeled with the scattering factor for neutral iron.

proceeds by chemical methods (I_2/AN), the solution is usually stirred vigorously for 2–3 days. This ensures good chemical contact of each cathode particle with iodine such that delithiation proceeds to completion.

Figures 5 and 6 show scanning calorimeter traces on hexagonal $Cu_{2/3}FeS_2$ and hexagonal $CuFeS_2$, respectively. Diffraction patterns of $Cu_{2/3}FeS_2$ samples cooled from 355 °C show that the products of the exothermic reaction near 205 °C are chalcopyrite, $CuFeS_2$, and marcasite, FeS_2. The reaction can be described by

$$Cu_{2/3}FeS_2\ (\text{hexagonal}) \rightarrow \underset{(\text{chalcopyrite})}{\tfrac{2}{3}\ CuFeS_2\ (\text{tetragonal})} + \underset{(\text{marcasite})}{\tfrac{1}{3}\ FeS_2\ (\text{orthorhombic})}\ . \quad (1)$$

Samples which have been cooled from 447 °C or 550 °C show diffraction patterns of chalcopyrite, and FeS_2, which is present as a mixture of marcasite and pyrite. Both thermograms show a small endothermic peak near 118 °C which corresponds to the melting of elemental sulfur which is present in less than 1%.

The general features observed in the thermogram of $Cu_{2/3}FeS_2$ are also observed for $CuFeS_2$ (hexagonal). The exothermic reaction which occurred near 205 °C now occurs near 340 °C. The diffraction pattern of $CuFeS_2$ (hexagonal), which had been heated to 365 °C or 550 °C, displays the powder pattern of chalcopyrite. Thus, it is evident that the layered Cu_xFeS_2 phase is a metastable phase at room temperature. It undergoes phase transitions to form pyrite or marcasite and chalcopyrite at elevated temperatures.

To understand the phase transition,

$$CuFeS_2\ (\text{hexagonal}) \rightarrow CuFeS_2\ (\text{tetragonal})\ , \quad (2)$$

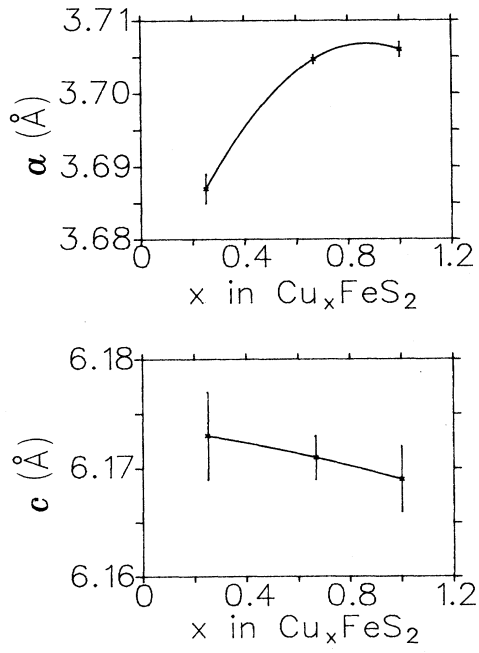

FIG. 3. Variation of the lattice parameters a and c in Cu_xFeS_2 with x.

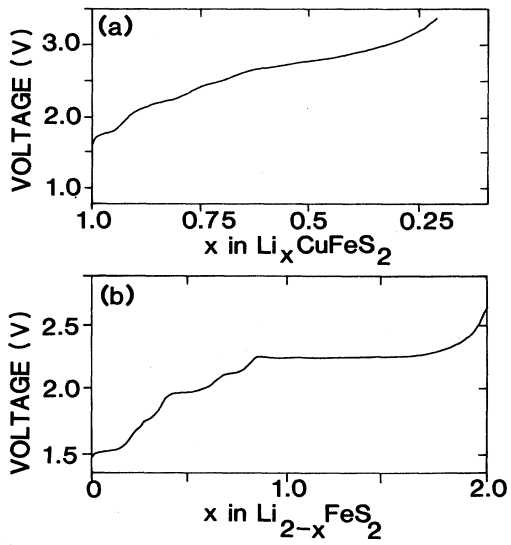

FIG. 4. A comparison of the recharge of (a), a $Li/LiCuFeS_2$ cell to 3.40 V, and (b) a Li/Li_2FeS_2 cell to 2.80 V. Both of these cells are charged at a rate of 20 h for 1 Li/Fe.

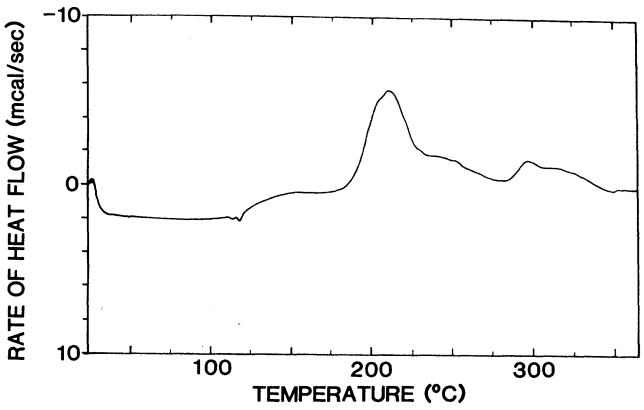

FIG. 5. Scanning calorimeter trace from a 33-mg sample of hexagonal $Cu_{2/3}FeS_2$ heated at a rate of 10 °C/min.

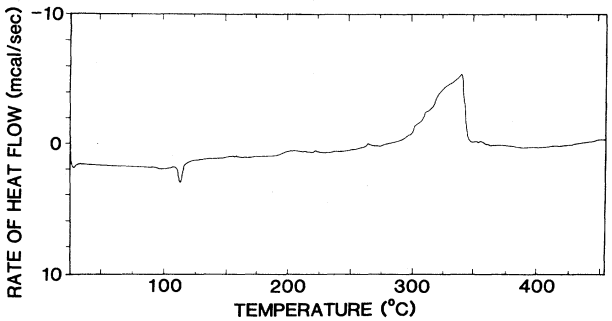

FIG. 6. Scanning calorimeter trace from a 26-mg sample of hexagonal $CuFeS_2$ heated at a rate of 10 °C/min.

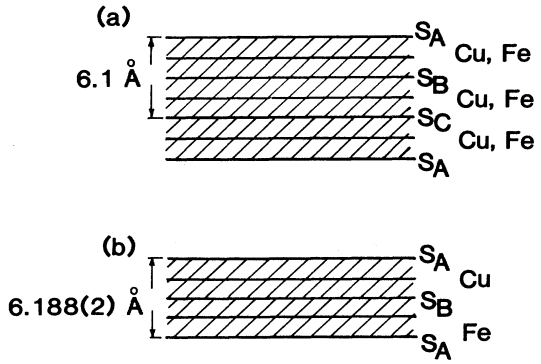

FIG. 7. A schematic diagram of the stacking sequence of (a) chalcopyrite in the [112] direction and (b) hexagonal $CuFeS_2$.

at elevated temperatures, the structure of chalcopyrite must be considered. Chalcopyrite contains four $CuFeS_2$ units in a tetragonal unit cell with $a=5.24$ Å, and $c=10.30$ Å.[10] In the [112] direction, the structure consists of layers of metal atoms sandwiched between planes of sulfur atoms, which are approximately cubic closed packed. The closest intraplanar S · · · S distance is 3.71 Å. In the notation of close-packed layers, chalcopyrite has a three-layer sulfur stacking sequence, and can be described by the stacking symbol

$$AaBbCc\ ,$$

where the upper case letters denote the relative sequence of the sulfur layers, and the lower case letters represent the Cu and Fe atoms in a 1:1 ratio occupying, in an ordered arrangement, half of the tetrahedral sites between two layers of sulfur.

From powder x-ray diffraction, the hexagonal $CuFeS_2$ phase has a unit cell dimension of $a=3.708(1)$ Å and $c=6.188(2)$ Å. The major difference in the arrangement of metal atoms of the metastable phase and chalcopyrite is shown schematically in Fig. 7. Assuming only Cu atom migration, we infer that the Cu and Fe atoms of the metastable phase do not reside between the same layers of sulfur. Instead, the Cu and Fe atoms occupy the tetrahedral sites in alternating layers of sulfur.

CONCLUSIONS

When copper atoms are substituted for lithium in Li_2FeS_2, a solid solution, $Li_{2-x}Cu_xFeS_2$ where $0 \le x \le 1$, forms. Single-crystal x-ray diffraction shows $LiCuFeS_2$ to be isostructural to Li_2FeS_2. Between two hexagonal close-packed sulfur layers, all the tetrahedral sites are filled equally and randomly with iron and copper. The lithium atoms fill the octahedral interstices between the alternate pair of sulfur layers.

Upon delithiation of the solid solution, either chemically or electrochemically, a hexagonal Cu_xFeS_2 ($\sim 0.25 < x \le 1$) phase forms. The crystal structure determination of a partially delithiated phase, $Li_{1-\delta}CuFeS_2$, where $\delta = 0.35 \pm 0.02$, shows that as lithium is removed, copper atoms diffuse into the tetrahedral sites of the lithium layer. Scanning calorimetry shows that the Cu_xFeS_2 ($\sim 0.25 < x \le 1$) phase is metastable, and upon heating, phase transitions back to the minerals, chalcopyrite and pyrite, occur.

ACKNOWLEDGMENTS

One of the authors (R. Fong) thanks the British Columbia Science Council (BCSC) for scholarship support. Part of this work was supported by the BCSC under Contract No. RC-13.

[1]S. Preto, Z. Tomczuk, S. von Winbush, and M. C. Roche, J. Electrochem. Soc. **130**, 264 (1983).
[2]R. J. Batchelor, F. W. B. Einstein, C. H. W. Jones, R. Fong, and J. R. Dahn, Phys. Rev. B **37**, 3699 (1988).
[3]R. Brec and A. Dugast, Mater. Res. Bull. **15**, 619 (1980).
[4]R. Fong, J. R. Dahn, and C. H. W. Jones (unpublished).
[5]C. A. Melandres and B. Tani, J. Phys. Chem. **82**, 2850 (1978).
[6]S. P. S. Badwal and R. J. Thorn, J. Solid State Chem. **43**, 163 (1982).
[7]*International Tables for X-ray Crystallography,* edited by J. A. Ibers and W. C. Hamilton (Kynoch, Birmingham, 1974), Vol. IV, Tables 2.2B and 2.3.1.
[8]E. J. Gabe, A. C. Larson, F. L. Lee, and Y. LePage, *NRC VAX Crystal Structure System* (National Research Council, Ottawa, 1984).
[9]W. R. McKinnon and J. R. Dahn, Solid State Commun. **52**, 245 (1984).
[10]R. W. G. Wyckoff, *Crystal Structures* (Interscience, New York, 1960), Vol. 2.
[11]A. C. T. North, D. C. Philips, and F. S. Mathews, Acta Crystallogr. **A24**, 351 (1968).
[12]J. DeMeulenaer and H. Tompa, Acta Crystallogr. **19**, 1014 (1965).